



Adaptive Minimal Control Synthesis for Satellite Attitude Control in Presence of Propellant Sloshing and Flexible Appendices*

Mario Cassaro, Jean-Marc Biannic, Hélène Evain

► To cite this version:

Mario Cassaro, Jean-Marc Biannic, Hélène Evain. Adaptive Minimal Control Synthesis for Satellite Attitude Control in Presence of Propellant Sloshing and Flexible Appendices*. European Control Conference ECC 2022, Jul 2022, Londres, United Kingdom. hal-03771813

HAL Id: hal-03771813

<https://hal.science/hal-03771813>

Submitted on 7 Sep 2022

HAL is a multi-disciplinary open access archive for the deposit and dissemination of scientific research documents, whether they are published or not. The documents may come from teaching and research institutions in France or abroad, or from public or private research centers.

L'archive ouverte pluridisciplinaire **HAL**, est destinée au dépôt et à la diffusion de documents scientifiques de niveau recherche, publiés ou non, émanant des établissements d'enseignement et de recherche français ou étrangers, des laboratoires publics ou privés.

Adaptive Minimal Control Synthesis for Satellite Attitude Control in Presence of Propellant Sloshing and Flexible Appendices*

Mario Cassaro¹, Jean-Marc Biannic¹ and Hélène Evain²

Abstract—In a scenario of always more complex and demanding space missions, enhanced attitude control systems play a key role for satellite design and capabilities improvement. In this paper, an adaptive and robust solution to the pointing angle tracking problem under mixed sources of disturbances is presented. A valid simplified parametric model, of a single axis satellite dynamics, is firstly introduced and discussed, to the objective of effectively accounting for propellant slosh and flexible appendices torque perturbations. The control problem is subsequently solved with a model reference adaptive control approach, namely the Minimal Control Synthesis (MCS). Theoretical fundamentals, architecture implementation and final tuning are reported. A subset of the extensive validation campaign performed is presented and discussed to demonstrate the impressive robustness and performance level reached by the proposed scheme. Limitations and future perspective to tackle them conclude the paper.

I. INTRODUCTION

Among the multiple sources of disturbance that can possibly compromise a geostationary satellite stability or jeopardize an interplanetary mission integrity, those generated by the propellant sloshing, together with the flexible appendices oscillations and their eventual mutual interaction remain the most critical, especially when dealing with active attitude control [1]. Propellant mass can reach up to approximately 40% of the entire satellite, [2], and to prevent its dangerous high-amplitude/slow-frequency motion, different passive physical solutions, such as baffles, compartmentalization or bladders are commonly employed [3]. However, physical suppression techniques increase mass, complexity, and cost of the overall system. For these reasons, novel active control system solutions are of great interest and remain an active research field, having fostered in the last decades multiple experiments aimed to obtain a more accurate understanding of the slosh phenomenon in zero gravity conditions [4], [5]. Based on recent advances in slosh modeling [6], CNES is funding, for few years now, a joint research program* in collaboration with the French Aerospace Lab (ONERA) in the attempt of investigating novel active control architecture capable of rejecting important amount of disturbances, while maintaining optimal tracking performances in terms of attitude control.

In this framework, while preliminary results on Low Earth Orbit (LEO) small-sized satellites were very promising, reaction wheels saturation and coupling dynamics with flexible appendices remain unresolved issues [7], [8]. These dynamics can no longer be neglected in the case of geostationary (GEO) or interplanetary mission satellites, which are typically equipped with significantly larger solar arrays structures and propellant tanks.

The purpose of the proposed paper is twofold: integrating sloshing and flexible modes dynamics in a unique, low complexity but accurate, satellite mathematical model; and derive an efficient control law solution, responding to disturbance rejection and tracking performance specifications while meeting saturation constraints.

The authors propose here to build a new single-axis satellite model, easily configurable, by integrating slosh and flexible modes, similar to what has been proposed in the *Demeter* benchmark, [9]. From a control perspective, justified by the intrinsic nonlinear and time varying nature of the system, the authors decide to investigate the potentiality of an adaptive control scheme in the attempt of deriving a single architecture capable of meeting performance and robustness criteria for the wide range of working conditions characterizing the problem at hand. In particular, an adaptive scheme, based on the Minimal Control Synthesis (MCS) theory, is derived, implemented and validated in simulation environment. MCS, firstly proposed by Stoten and Benchoubane [10], [11], is a significant extension to model reference adaptive control (MRAC) [12], which working principle is to regulate the error between a nonlinear, possibly unstable, time variant, partially or fully unknown plant with respect to a desired, linear time-invariant stable dynamics, namely *reference model*. What attracted the authors attention to the MCS techniques is: the absence of need for plant model identification, apart from the general structure of the state-space representation; the capability for compensating for a large bandwidth of external disturbances; the low computational burden; and the easy parallelization with other control laws. All these properties perfectly respond to the requirements of the control objective under analysis, and are investigated in detail. The article is organized as follows. In Section II, the flexible satellite model is fully described. Next, the control problem is presented in Section III and solved in Section IV with the MCS approach which is first briefly described. In section V the obtained results are commented. Finally, some concluding comments and research perspectives end the paper.

*This work was supported by CNES, COSOR program

¹Mario Cassaro and Jean-Marc Biannic are with the Département Traitement de l'information et systèmes, DTIS, at ONERA, Toulouse, France mario.cassaro@onera.fr, jean-marc.biannic@onera.fr

²Hélène Evain is with CNES, Toulouse, France Helene.Evain@cnes.fr

II. SATELLITE MODEL INCLUDING SLOSHING AND FLEXIBLE APPENDICES

To the objective of deriving satellite's attitude control laws tolerant to multiple sources of perturbations a suitable modeling formulation is hereafter proposed integrating propellant sloshing and flexible solar panels dynamics to the rigid body satellite equations with actuation constraints. With reference to Fig. 1, considering, as a start, the sloshing mode parameters fixed over time (implicit temporal variations will be introduced subsequently) the satellite main rotational equilibrium equation about a single-axis is simply given by:

$$J\ddot{\theta} = T_W + T_F + T_S + T_D \quad (1)$$

where, as from standard nomenclature, θ is the satellite attitude in $[rad]$, J the satellite inertia about the axis in $[Kg \cdot m^2]$ and the external torque, acting on the system, is expressed as a summation of the four components, respectively the reaction wheel (T_W), the flexible appendices (T_F), the propellant slosh (T_S) and a generic external disturbance (T_D). T_W represents the control torque, exerted by a single reaction wheel and modeled as a simple first order dynamics with a time constant of $\tau = 0.5[s]$, expressed as

$$H_W = sat_{T_{max}}(T_C)/s \quad (2)$$

$$T_W = sat_{H_{max}}(H_W) \frac{s}{1 + \tau s}. \quad (3)$$

The reaction wheel actuation device is physically limited in acceleration, bounding the torque generation range, and velocity, constraining the maximum reachable kinetic momentum. Both limitations are modeled as simple signal saturation in (2) and (3), however, while constraining $|T_C| < T_{max}$ simply reduces the control authority to a certain value, imposing $|H_W| < H_{max}$ causes a sudden fall of the control torque to zero when the wheel maximum rotational speed is reached since no extra acceleration is possible. This is mathematically expressed in equation (3) by the derivative of a constant term ($\pm H_{max}$) which clearly equals zero.

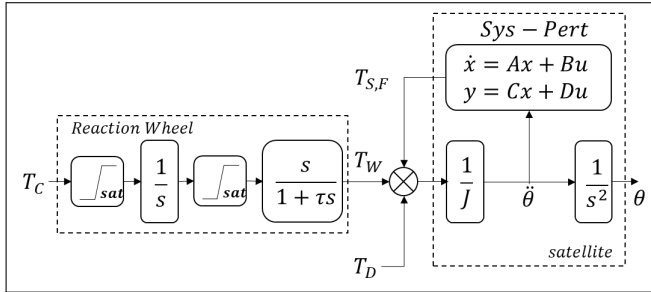


Fig. 1. Complete satellite block model

A. Sloshing and Flexible Dynamics Modeling

Based on outcomes of previous researches summarized in [7], the sloshing propellant torque can be modeled as the superposition of nonlinear, time-varying, poorly damped and low-frequency second order dynamics.

Assuming the fluid initially at rest, and considering its mass variation negligible during a single maneuver [13], a unique, more classical formulation, based on the Cantilever Hybrid Model analogy, proposed in [14], can be employed both for slosh and flexible appendices dynamics description

$$T_{Si} = \frac{s^2}{s^2 + 2\xi_{Si}\omega_{Si}s + \omega_{Si}^2} L_{Si} \ddot{\theta} \quad (4)$$

$$T_{Fi} = \frac{s^2}{s^2 + 2\xi_{Fi}\omega_{Fi}s + \omega_{Fi}^2} L_{Fi} \ddot{\theta} \quad (5)$$

where $L_{S/Fi}$, $\omega_{S/Fi} = \sqrt{c_{S/Fi}}$ and $\xi_{S/Fi} = \frac{k_{S/Fi}}{2\sqrt{c_{S/Fi}}}$ respectively denote the slosh/flexible modal contribution, the pulsation and the damping coefficient of the i^{th} slosh/flexible mode. From available experimental data analysis, [15], the three different slosh modes are chosen as fixed parameters in the following intervals: $\omega_{Si} \in [0.1, 0.3]$, $\xi_{Si} \in [0.001, 0.03]$ and $L_{Si} \in [30, 50]$. While flexible proper frequencies and damping ratio are chosen as: $\omega_{Fi} \in [0.6, 10]$, $\xi_{Fi} \in [10^{-4}, 10^{-3}]$ and $L_{Fi} \in [50, 300]$. This representation allows for easily manipulating the slosh/flexible frequency characteristics and analyze the control law robustness against modeling uncertainties.

Remark 1: Usual values for the first flexible mode proper frequency, of a similar configuration satellite, are often in the range $\omega_F \in [1, 3][rad/s]$. Here, a slightly smaller lower-bound is considered to trigger and analyze potential interactions between the two phenomena.

B. Implementation and Open-Loop Analysis

The second order transfer functions describing the perturbations' dynamics have been manipulated and rearranged to be uniform in terms of input/output configuration to the objective of applying superposition principle and lump the entire set of external torque effects in a single state-space representation, namely *Sys-Pert* in Fig.1. Following standard nomenclature, *Sys-Pert* has input $u = \ddot{\theta} \in \mathbb{R}^{1 \times 1}$, output $y = T_{S,F} \in \mathbb{R}^{1 \times 1}$, state matrix $A_{S,F} \in \mathbb{R}^{14 \times 14}$, which eigenvalues correspond to the 2×7 roots of the defined transfer function denominators, control matrix $B_{S,F} \in \mathbb{R}^{14 \times 1}$, observation matrix $C_{S,F} \in \mathbb{R}^{1 \times 14}$ and the feedthrough matrix $D_{S,F} \in \mathbb{R}^{1 \times 1}$. The general equation of the complete satellite (1), respecting the systems interconnection reported in Fig. 1, is hence rewritten including the perturbations effect in the following state-space form:

$$\dot{x}_{sat}(t) = A_{sat}(\Lambda)x_{sat}(t) + B_{sat,S,F,W}[T_W(t), T_{S,F}(t), T_D(t)]^T \quad (6)$$

$$y_{sat}(t) = C_{sat}x_{sat}(t) \quad (7)$$

where $x_{sat} = [\theta, \dot{\theta}, x_{S,F}, x_W]^T \in \mathbb{R}^{17 \times 1}$ is the complete satellite state vector including the 2 rigid body, the 14 *Sys-Pert* and the single actuation states; $A_{sat}(\Lambda) \in \mathbb{R}^{17 \times 17}$, is the extended state matrix depending on the chosen values of $\Lambda = [\omega_{S,Fi}, \xi_{S,Fi}, L_{S,Fi}]$, $B_{sat} \in \mathbb{R}^{17 \times 3}$, is the extended control

matrix and $C_{sat} = [I^{2 \times 2} | 0^{2 \times 15}]$ the extended output matrix. The satellite inertia is fixed at $J = 1000 [Kg \cdot m^2]$. The maximum torque attainable by the reaction wheel is fixed at $T_{max} = 0.5 [N]$ and its maximum angular momentum is $H_{max} = 10 [N \cdot m \cdot s]$.

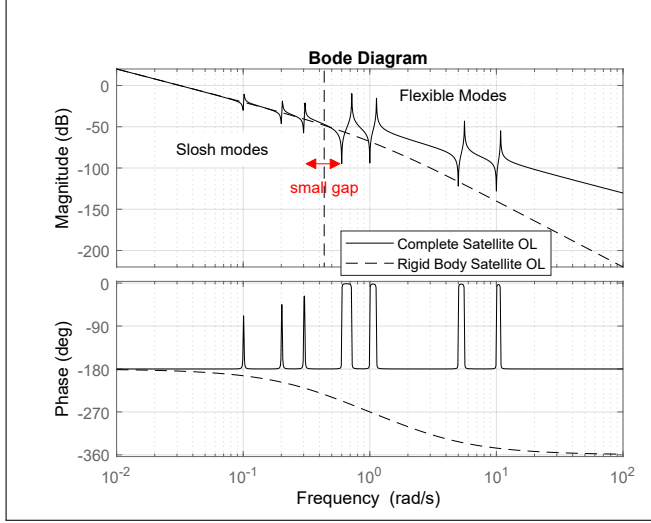


Fig. 2. Model Open-Loop Analysis

The frequency domain characteristics of the so modeled *Rigid Satellite* and *Complete Satellite* open-loops, for a single configuration of *Sys-Pert*, are reported in Fig. 2, in the form of a *bode* diagram. While the dynamic response remains unchanged at very low frequencies, where the two integrators represent the dominant poles, the rigid dynamics is modified by the presence of the sloshing modes, for frequencies comprise in $0.1 < \omega_{Si} < 0.3 [rad/s]$, and by the flexible modes, for frequencies comprise in $0.6 < \omega_{Fi} < 10 [rad/s]$. As previously discussed, the small gap between the two extremes resonant peak has been chosen to induce interactions between the modes and evaluate the controller robustness in such critical conditions.

III. CONTROL OBJECTIVE AND PROBLEM FORMULATION

The control objective is to drive the satellite attitude angle θ to any constant set point, while suppressing oscillatory motion induced by propellant sloshing and flexible appendices modes, and adaptively compensating for uncertainties in *Sys-Pert* parameters and model's nonlinearities. In this particular development, it is assumed that the only system's measurements available for feedback are $y_{sat} = x_{meas} = [\theta, \dot{\theta}]^T$, where perfect sensors hypothesis holds. Performance specifications, which are considerably demanding for space application, set a maximum stationary residual tracking error of $\theta_e \leq 0.04 [deg]$, and a steady-state velocity error of $\dot{\theta} \leq 0.1 [deg/s]$. Actuation saturation should be avoided or at least should not jeopardize performances.

As discussed in Sec. II, the physical system under analysis can be modeled as multiple LTI system for different Λ values leading to the formulation reported in Eqs. (6) and (7). To the objective of designing a model reference control law, both

representations can be considered as sub-classes of a more general continuous-time, nonlinear and eventually unknown plant description, which can be expressed in an amenable form as:

$$\dot{x}(t) = Ax(t) + Bu(t) + d(t) \quad (8)$$

where $x(t)$ is the state vector, $x \in \mathbb{R}^n$, $u(t)$ is the control input, $u \in \mathbb{R}^m$, A and B are the state and control linear time invariant (LTI) components of the complete plant dynamics, $A \in \mathbb{R}^{n \times n}$ and $B \in \mathbb{R}^{n \times m}$, and $d(t)$ gathers all the nonlinearities, parameters variations, unknown/unmodeled dynamics and disturbances. For a general model reference control scheme, the control problem lies in choosing $u(t)$ such that all the states $x(t)$ in the closed-loop system are uniformly bounded and track the state vector of a desired reference model, both in transient and in steady-state for any bounded reference signal $r(t)$.

$$\dot{x}_m(t) = A_m x_m(t) + B_m r(t) \quad (9)$$

where $x_m(t)$ and $r(t)$ are congruent in dimension with $x(t)$ and $u(t)$ respectively.

IV. MINIMAL CONTROL SYNTHESIS

A. Theoretical Preliminaries

The general architecture of a direct adaptive control scheme for a tracking control problem is reported in Fig. 3 and serves as reference for the following discussion as it is valid both for MRAC and MCS control algorithms. As a matter of fact, the MCS formulation consists in a variation of an MRAC formulation reported in [12].

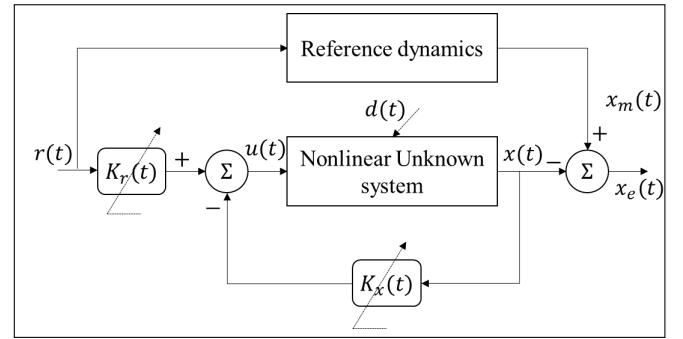


Fig. 3. General Direct Adaptive Control Scheme for tracking control problem

The control signal $u(t)$, in the direct adaptive MRAC algorithm, is obtained as a function of the plant states and the reference signal

$$u(t) = -(K_x - k_x(t))x(t) + (K_r + k_r(t))r(t) \quad (10)$$

where K_x and K_r are constant feedback and feedforward gain matrices, which can be computed by matrix inversion in their closed form; while $k_x(t)$ and $k_r(t)$ are the so called adaptive gains, which specific but not unique solution respecting hyper-stability criterion is obtained in [12], and written as:

$$k_x(t) = \int_0^t \alpha y_e(\tau) x^T(\tau) d\tau + \beta y_e(t) x^T(t) \quad (11)$$

$$k_r(t) = \int_0^t \alpha y_e(\tau) r^T(\tau) d\tau + \beta y_e(t) r^T(t) \quad (12)$$

where the first integral terms assure the memory of the adaptive system, while the second terms characterize the transient response vanishing for $y_e(t)$ and $r(t)$ going to zero. The integral terms are also stabilizing solutions, obtained solving the adaptive problem with a, strictly positive real, SPR-Lyapunov approach, as reported in [11]. In Eq. 11 and 12 α and β are tuning parameters, and $y_e(t)$ is the output error signal, defined as

$$y_e(t) = C_e x_e(t) \quad (13)$$

where

$$C_e = B^T P \quad (14)$$

and P is the positive definite solution of the Lyapunov equation, for guaranteeing stability, which depends only on the chosen reference dynamics:

$$A_m^T P + P A_m = -Q; \quad Q > 0 \quad (15)$$

This formulation however implies a knowledge of the B matrix, and A matrix for the constant gains calculation, recalling to be the linear parts of the unknown nonlinear system control matrices, and so forth requires some equations manipulation. Based on these results, Stoten and Benchoubane in [10], proposed to assume null constant gains components, *i.e.* $K_x = K_r = 0$, and that everything except the general structure of the plant (*i.e.* the number of degrees of freedom and state dimension) are unknown.

Thus, eq. (10), becomes

$$u(t) = k_x(t)x(t) + k_r(t)r(t) \quad (16)$$

and the C_e matrix in the output error equation (13), is modified by employing the horizontal companion form of A_m and obtained as

$$C_e = \bar{C} P \quad (17)$$

where P remains the positive definite solution of the Lyapunov equation and $\bar{C} = [0 \dots 0 \quad 1]^T$. This conceptually frees the designer from any plant knowledge and equation manipulation, while maintaining convergence guaranties. Proofs of stability can be found in related literature, and omitted here for sake of brevity.

Another improvement is proposed with the aim of rejecting constant disturbances and plant biases leading to static error of the Eq.(16) control law. It consists of enriching the control signal by another adaptive gain, reproducing some sort of integral action into the adaptive algorithm. The new control law is written as

$$u(t) = k_x(t)x(t) + k_r(t)r(t) + k_i(t)x_i(t) \quad (18)$$

where

$$k_i(t) = \int_0^t \alpha y_e(\tau) x_i^T(\tau) d\tau + \beta y_e(t) x_i(t) \quad (19)$$

and

$$x_i(t) = \int_0^t [r(\tau) - y(\tau)] d\tau; \quad y(t) = Cx(t) \quad (20)$$

The so written control law still verify Popov hyperstability criterion and guarantees convergence with and without locked gains as reported in the relative literature.

B. Implementation

The first step for the implementation of a model reference control technique is the choice of a suitable reference dynamics, which is of critical importance depending on the system's nature. A typical example concerns the demanded level of performance, which if unrealistic and unattainable could jeopardize the dynamic response of the overall system if not accounted for in the early steps of the reference model design. As described in Sec. II and III, for the problem under investigation major limitations are imparted by the actuation system and its critical behavior when the wheel's maximum acceleration is reached and the supplied torque falls to zero. For this reason, to guarantee reachability of the demanded performances, the reference model is chosen to be a stable closed-loop dynamics of the equivalent rigid satellite, with the same physical characteristics, controlled by a H_∞ tuned PID. The resulting state and control matrices, reported in Eq.(21), describe a reference dynamics characterized by a damping ratio at $\zeta = 0.75$ and a proper frequency of $\omega_n = 0.5$ [rad/s]. It is worth mentioning that including the actuator filter, for the reference model computation, would only have produced a minor right shift of the dominant poles, which justifies its negligibility without loss of generality nor performances. The use of a second order reference model to control a higher order plant (17 for the case being) is common practice. It depends on the control problem formulation and the observability and controllability characteristics of the system. Here, only the dominant observable dynamics is being imposed, *i.e.* $x = [\theta, \dot{\theta}]$, hence a second order reference model suffices to the desired control purpose.

The final design parameters are obtained and hereafter reported for the *Reference Model*

$$A_m = \begin{pmatrix} 0 & 1 \\ -0.0025 & -0.075 \end{pmatrix}; \quad B_m = \begin{pmatrix} 0 \\ 0.0025 \end{pmatrix}; \quad (21)$$

and the *Adaptation Mechanism*

$$\alpha = 0.01 \quad \beta = 100 \quad (22)$$

and choosing $Q = I(2 \times 2)$ the solution of the Lyapunov equation, $A_m^T P + P A_m = -Q$ returns $C_e = [200 \quad 2673]$.

V. RESULTS AND DISCUSSION

An extensive validation campaign, (≈ 10000) runs, is performed in different simulation scenarios to the objective of evaluating general performances and robustness of the proposed adaptive control scheme in nominal and off-nominal conditions, analyzing the overall system behavior, if inertial wheel saturation is reached or not. Only the most meaningful are reported in the article for the sake of space. The two types of maneuvers for which a satellite attitude controller is designed are a *step*, single rotation to reach a certain pointing angle, and a *square wave*, back and forward rotation around the axis to track varying orientation commands. The amplitude of the demanded rotation could eventually lead to wheel saturation and consequent instability, this justifies the need of verifying the system behavior for small and large amplitude angle demand. Perturbations of different nature are considered, separately and jointly, to initially investigate the rejection performances of the proposed control law. Robustness is verified against propellant mass variation and structural uncertainties. This translates in modeling a random, uncorrelated, normally distributed, zero mean, frequency shift of the resonant peaks both for the slosh and the flexible modes. Standard deviations varies accordingly with test-defined level of uncertainties (*i.e.* 25 – 50%).

Only results for the most challenging test setup are presented here in Fig.4, with the objective of giving an insight of the robustness and adaptive capabilities of the proposed control scheme. A set of 50 simulations, for the tracking problem of a square wave, with randomly varying uncertainties on ω_{S_i} and ω_{F_i} in the range of $\pm 50\%$ is reported. Fig.4 displays, from the top: the states response time histories; the control action, in terms of commanded vs. executed torque, and the reaction wheel momentum, where different colors refer to different simulation runs as for the following; the evolution of the adaptive gains; and finally the separated contributions of the perturbation torques. From this last, the changing frequencies content of the disturbances and the random nature of their combination can be appreciated. Despite the conditions' severity, the designed control law remains capable of compensating for all nonlinearities and varying dynamics thanks to the sufficiently fast dynamics of the adaptive gains. While K_x and K_r , drastically converge after 260[s], when θ_c returns to zero, the integral gain K_i continues to vary guaranteeing steady-state performance while compensating for residual slosh and flexible perturbations. This confirms the need of an integral action.

The actuator, reveals an extremely intense activity, which should be evaluated in terms of energy consumption. However, saturation is only reached once, for a very limited period of time, in the first maneuver without compromising nor performance nor stability. Finally, but most importantly, the strong potentiality of the control scheme can be appreciated looking at the satellite states, which are practically overlapped for the entire set of simulation, excepted for small differences in $\ddot{\theta}$. Performance and robustness can be considered verified and very satisfactory.

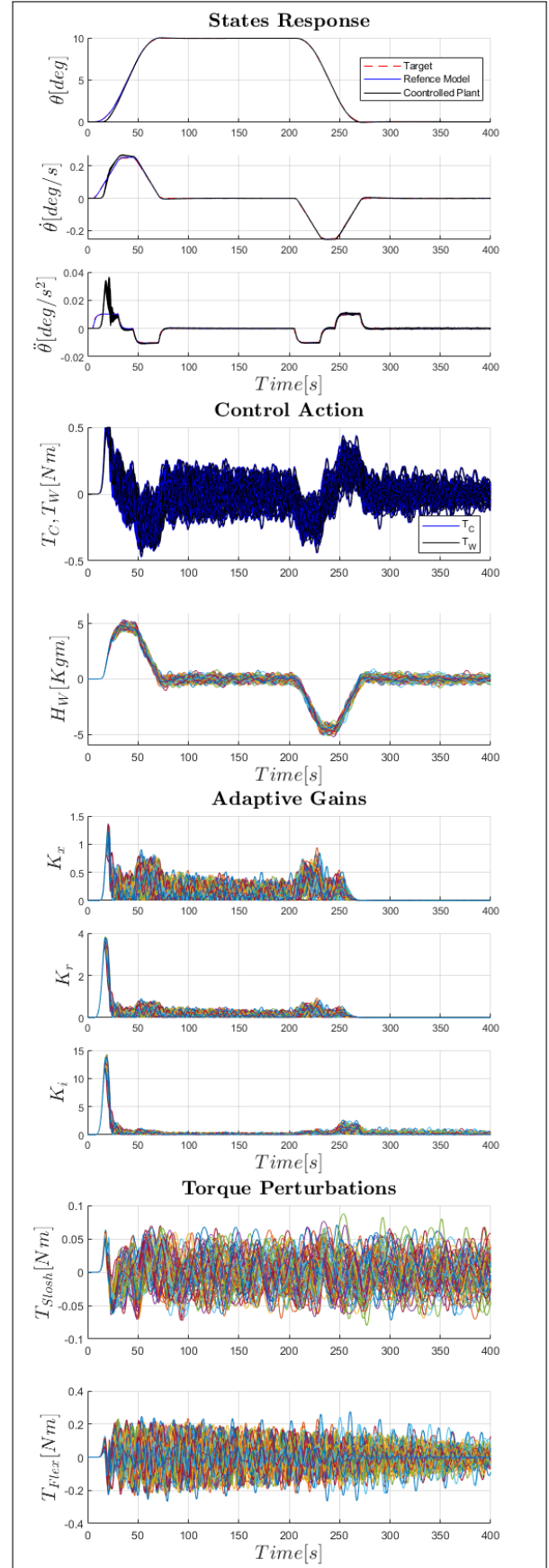


Fig. 4. Closed-loop analysis

To the objective of seeking for closed-loop system limitations, the control law is exposed to long lasting actuator saturation by demanding increasingly high attitude set points. Results reported in Fig. 5. In contrast with the previously investigated control solutions, [7] and [8], where the closed-loop system resulted incapable of recovering from instability consequent to actuation torque saturation, starting at target angle $\theta_c \approx 10[\text{deg}]$; obtained results, for the proposed adaptive control strategy, confirm that even for long lasting saturation of the wheel, system convergence is still guaranteed both for large step and square wave, omitted here, tracking signal. However, a larger overshoot, and longer settling time, impossible to counteract due to the actuation system limitations, characterize the time response leading to unacceptable performances, starting at $\theta_c = 25[\text{deg}]$. An easy overcome to this issue is a discretization of the trajectory, as subsequent step of $20[\text{deg}]$ maximum, which will allow to rotate the satellite indefinitely maintaining the optimal level of performance, robustness and adaptation. A more elegant solution, will consist in coupling the proposed control law with an input shaping scheme, which is part of the research future perspectives.

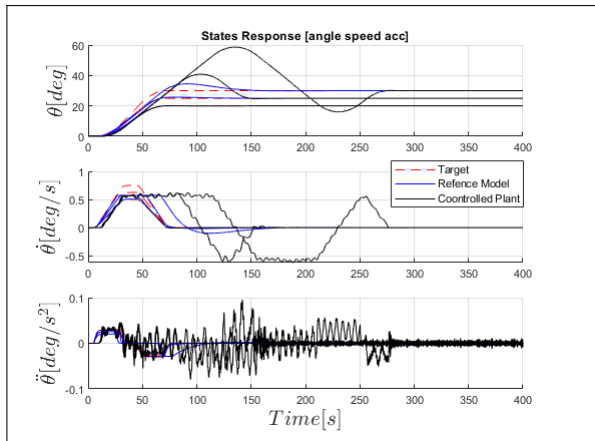


Fig. 5. Test setup: C.4.I, Large Pointing Error Behavior

VI. CONCLUSIONS

Based on recent advances in propellant slosh modeling a valid, simple parametric LTI model, of a single axis satellite dynamics, accounting for both slosh and flexible appendices has been derived and implemented. An adaptive and robust control solution, based on Minimal Control Synthesis theory, for the pointing error tracking control problem has been proposed and implementation details are given to the reader. The extensive validation campaign performed, of which only the most meaningful results have been reported, demonstrated impressive robustness and performance level. Mutual combination and interaction of propellant slosh and flexible appendices dynamics have been successfully damped out while maintaining demanded pointing angle accuracy. The unique drawback of the proposed control scheme lies in the impossibility of accounting for saturation constraints other than reducing model reference dynamics performance, which

de facto limits the amplitude of the maximum demanded rotation. The apparently severe limitation can be overcome by taking advantage of the decentralized MCS properties [16], which allows to implement the adaptive control scheme in parallel to any other conventional controller. A coupling with an input shaping control strategy is hence foreseen by the authors as future perspective.

REFERENCES

- [1] M. Juanpere, A. Dalmon, P. Regnier, P. Laurens, H. Bavestrello, and J. Levenhagen, "Sloshing aocs/fluidic coupled analysis," in *ESA GNC 2021*, 2021.
- [2] C. Russell, F. Capaccioni, A. Coradini, M. De Sanctis, W. Feldman, R. Jaumann, H. Keller, T. McCord, L. McFadden, S. Mottola, *et al.*, "Dawn mission to Vesta and Ceres," *Earth, Moon, and Planets*, vol. 101, no. 1, pp. 65–91, 2007.
- [3] A. G. de Souza and L. C. de Souza, "Design of satellite attitude control system considering the interaction between fuel slosh and flexible dynamics during the system parameters estimation," in *Applied Mechanics and Materials*, vol. 706. Trans Tech Publ, 2015, pp. 14–24.
- [4] S. Chintalapati, C. Hollicker, R. Schulman, E. Contreras, H. Gutierrez, and D. Kirk, "Design of an experimental platform for acquisition of liquid slosh data aboard the International Space Station," in *48th AIAA/ASME/SAE/ASEE Joint Propulsion Conference & Exhibit*, 2012, p. 4297.
- [5] J. Mignot, R. Pierre, M. Berhanu, B. Busset, R. Roumigué, H. Bavestrello, S. Bonfanti, T. Miquel, L. Marot, and A. Llodra-Perez, "Fluid dynamic in space experiment," in *68th International Astronautical Congress (IAC)*, Adelaide, Australia (IAC-17-A2. 62), 2017.
- [6] A. Dalmon, "Simulation numérique du ballonnement d'ergol et modélisation de l'interaction fluides-membrane dans un réservoir de satellite," 201.
- [7] J.-M. Biannic, A. Bourdelle, H. Evain, S. Moreno, and L. Burlion, "On robust LPV-based observation of fuel slosh dynamics for attitude control design," *IFAC-PapersOnLine*, vol. 52, no. 28, pp. 170 – 175, 2019, 3rd IFAC Workshop on Linear Parameter Varying Systems LPVS 2019. [Online]. Available: <http://www.sciencedirect.com/science/article/pii/S2405896319322694>
- [8] A. Bourdelle, J.-M. Biannic, H. Evain, S. Moreno, C. Pittet, and L. Burlion, "Propellant Sloshing Torque H_∞ -based Observer Design for Enhanced Attitude Control," *IFAC-PapersOnLine*, vol. 52, no. 12, pp. 286–291, 2019.
- [9] C. Pittet and D. Arzelier, "Demeter: A benchmark for robust analysis and control of the attitude of flexible micro satellites," *IFAC Proceedings Volumes*, vol. 39, no. 9, pp. 661–666, 2006.
- [10] D. Stoten and H. Benchoubane, "Empirical studies of an mrac algorithm with minimal controller synthesis," *International Journal of Control*, vol. 51, no. 4, pp. 823–849, 1990.
- [11] —, "Robustness of a minimal controller synthesis algorithm," *International Journal of Control*, vol. 51, no. 4, pp. 851–861, 1990.
- [12] I. Landau and B. Courtiol, "Design of multivariable adaptive model following control systems," *Automatica*, vol. 10, no. 5, pp. 483–494, 1974.
- [13] P. Mason and S. Starin, "The effects of propellant slosh dynamics on the solar dynamics observatory," in *AIAA Guidance, Navigation, and Control Conference*, 2011, p. 6731.
- [14] J.-P. Chretien and C. Manceaux-Cumer, "Minimal LFT form of a spacecraft built up from two bodies," in *AIAA Guidance, Navigation, and Control Conference and Exhibit*, 2001, p. 4350.
- [15] A. Bourdelle, L. Burlion, J.-M. Biannic, H. Evain, S. Moreno, C. Pittet, A. Dalmon, S. Tanguy, and T. Ahmed-Ali, "Towards New Controller Design Oriented Models of Propellant Sloshing in Observation Spacecraft," in *AIAA Scitech 2019 Forum*, 2019, p. 0115.
- [16] H. Benchoubane and D. Stoten, "The decentralized minimal controller synthesis algorithm," *International journal of control*, vol. 56, no. 4, pp. 967–983, 1992.